THERMAL-WAVE MEASUREMENTS OF MULTI-LAYER SUPERINSULATION FOILS

N. Marquardt, V. John, IBS-DELTA, University of Dortmund;
B.K. Bein, I. Delgadillo, A. Haj-Daoud, J. Gibkes, J. Pelzl, Exp. Phys. III, Ruhr University Bochum

Abstract

Thermal wave measurements rely on modulated laser heating and IR detection of the thermal response, using a MCT detector with IR optics and lock-in amplifier. Both, the amplitude and the phase retardation of the thermal wave response with respect to the heating modu-lation, provide information on the effective thermal transport properties of the measured samples. Here we apply this method to determine the shielding properties of multi-layer superinsulation foils, used for the thermal insulation of superconducting magnetic coils in particle accelerators, e.g. in LHC at CERN. The measurements, performed at ambient temperature and ambient and reduced pressure, have been interpreted using a theoreti-cal model, including both conductive and radiative heat transport. The results show that the radiative heat transport can be well identified, although the conductive heat transport is dominant across multi-layer samples. At reduced pressures, the conductive heat transport decrea-ses considerably and, depending on the number of spacer layers, the radiative heat transport can become dominant. Applying this new photothermal technique, the shielding efficiencies of multi-layer superinsulation foils have been compared in this work for the first time.

1 INTRODUCTION

Owing to voids, an effective low mass density and a relatively low thermal conductivity, the internal radiative heat transport can play an important role in heat insulation materials. Apart from foams and ceramics, such effects are also relevant in multi-layer superinsulation foils consisting of highly reflective aluminized mylar foils, which serve for the thermal insulation of e.g. space shuttles, satellites and superconducting magnetic coils. In large scale applications of superconductivity in particle accelerators or in Tokamak devices, e.g. in the Large Hadron Collider at CERN or in Tore Supra, the energy costs for cooling are relatively high and require optimization of the insulation system. This may be achieved by an appropriate number of insulation and spacer layers, by optimizing the thickness and homogeneity of the individual mylar layers, by optimizing the thickness and the reflection properties of the metal films, and by searching for a suitable material used for metallization.

Photothermal measurements based on modulated heating in the visible spectral range and IR detection of the thermal wave response are used here to determine the effective thermal transport properties or shielding properties of multi-layer superinsulation foils consisting of a different number of aluminized mylar layers and spacer layers. The measurements have been run both, at ambient pressure and at reduced pressures.

In chapter 2, the measurement method is briefly described, followed in chapter 3 by the results obtained at ambient pressure for different numbers of aluminized mylar foils and spacer layers of the superinsulation system Lydall Dam [*]. The results obtained at reduced pressures (1 mbar – 750 mbar) for a constant number of aluminized mylar layers and spacer layers are presented in chapter 4. The measured data are interpreted in the frame of a theory [1] for transmitted photothermal waves, considering both conductive and radiative heat transport.

2 INFRARED RADIOMETRY OF THERMAL WAVES

The present measurements and their interpretation are based on the transmission of thermal waves [1], where the front surface of the sample is heated and the thermal response is detected at the sample's rear surface. This method is especially suited to measure the insulation properties of samples of finite thickness and of layer systems with different numbers of layers.

The measuring system we developed for IR detection of thermal waves consists of 4 main components (Figure 1): an argon-ion laser (Spectra Physics Series 2000), to excite thermal waves of small temperature amplitude, a vacuum cell to keep the samples at a desired constant sample temperature, an IR detector to measure the IR emission, and a lock-in amplifier to filter the small periodical variations related to the thermal wave response

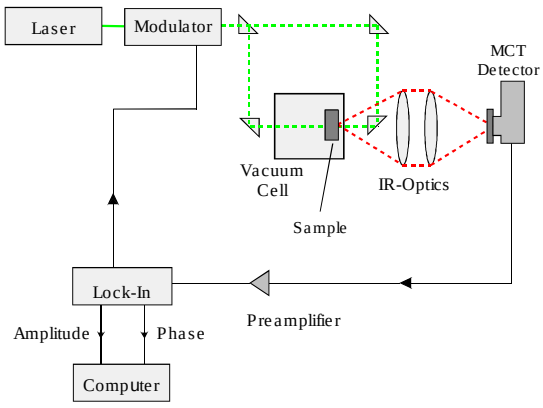

Figure 1: Scheme of thermal-wave detection in vacuum, in the transmission and reflection configuration.

from the high radiation level corresponding to the average sample temperature

For the present measurements the samples have been kept at ambient temperature, 20°C, and the pressure has been varied between 1 mbar and ambient pressure. The laser beam of nominal power of 1000 mW has been modulated with the help of an acousto-optic modulator (Isle Optic, LM 080) in the frequency range from 0.03 to 20 Hz. A large heating spot of about 10 mm has been used, to reduce the effects of lateral heat transport parallel to the metallized foils. For IR detection a MCT detector (Judson), BaF_2 lenses, and a cut-on filter are used which allow a detection interval of 1 µm – 12 µm and a maximum solid angle of 0.196 sr. Based on this detection system, thermal wave amplitudes as small as ΔT = 44 µK, 15 µK and 9 µK have been detected at sample temperatures of 300, 400, and 500 K [2].

For quantitative interpretation the signals have been calibrated by reference measurements, with the heated sample support or with samples of different numbers of insulation foils. Assuming IR opaque samples, the normalized amplitudes [1] are:

$$S_n = \left(\frac{S_s}{S_r}\right) = \left(\frac{\eta_s\, e_r}{\eta_r\, e_s}\right)\left[\frac{\exp(2\sqrt{\pi f\,\tau_r}) - 2\cos(2\sqrt{\pi f\,\tau_r}) + \exp(-2\sqrt{\pi f\,\tau_r})}{\exp(2\sqrt{\pi f\,\tau_s}) - 2\cos(2\sqrt{\pi f\,\tau_s}) + \exp(-2\sqrt{\pi f\,\tau_s})}\right]^{1/2},$$

where S_n is the normalized signal, S_s the signal of the foil of unknown properties and S_r the signal of the reference. The quantities η, e, and τ are the photothermal efficiency, thermal effusivity, and thermal diffusion time, respectively, and the indices s and r refer to the sample and the reference. The thermal diffusion time of reference and sample, are $\tau_{r,s} = d_{r,s}^{\,2} / \alpha_{r,s}$ where d is the sample thickness and α the effective thermal diffusivity. In the low-frequency limit, the above equation pro-vides information on the damping of the steady-state heat transport based on radiation and conduction by the various layers of the foils. The relative changes of the thermal diffusivity are obtained from the normalized phases:

$$\tan(\Phi_s - \Phi_r) = \frac{\tan(\sqrt{\pi f\,\tau_s})\cot(\sqrt{\pi f\,\tau_s}) - \tanh(\sqrt{\pi f\,\tau_r})\cot(\sqrt{\pi f\,\tau_r})}{1 + \tan(\sqrt{\pi f\,\tau_s})\cot(\sqrt{\pi f\,\tau_s})\tanh(\sqrt{\pi f\,\tau_r})\cot(\sqrt{\pi f\,\tau_r})}$$

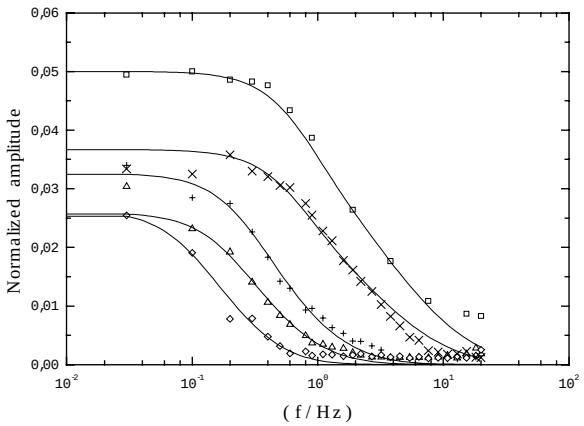

Figure 2: Normalized amplitudes of sandwich samples with different numbers of foils, compared with theory.

Additionally, some measurements have been interpreted using a more general thermal wave theory where both conductive and radiative heat transport are considered explicitely [3].

3 MEASUREMENTS AT AMBIENT PRESSURE

Subsequently we present the results of thermal wave measurements of the effective thermal transport properties of multi-layer superinsulation foils for the example of the multi-layer system Lydall DAM, one of the test samples provided by CERN, Geneva [*]. The multi-layer system Lydall DAM consists of external metallized mylar foils of 25 µm thickness both at the front and rear of the multi-layer system, in the interior spacer layers and metallized mylar foils of 6 µm thickness follow each other. Our measurements have been run on an external foil separately and on multi-layer systems consisting of the external foil at the front surface and up to seven sequences of spacer and internal metal foils. Here the results are discussed, which have been measured at ambient pressure and ambient temperature.

In the low frequency limit, the normalized amplitudes (Figure 2) give information on the attenuation of the incident steady state heat flux by the various foils. Thus, the heat flux is reduced by the external 25 µm thick metallized foil to a value of only 5% ( ), whereas for the composite insulations with the increasing number of spacer layers and internal foils (×, +, Δ) the steady state heat transport is reduced to values of about 4%, 3.5%, and 3%, respectively. For the sample with the additional external foil at the rear surface (◊), it is reduced to about 2.5%.

From the general agreement between measured data and theoretical approximation, we can conclude, that the main contributions to the heat transport are diffusive and that only the slight deviations at higher frequencies can be identified as radiative contributions.

4 MEASUREMENTS AT REDUCED PRESSURE

By using a vacuum cell at reduced air pressure, first measurements have been run for a sandwich system consisting of the external foil, a spacer layer and an internal foil. Consequently the data obtained at reduced pressure can be compared with the data represented by the symbol **x** in Figure 2. In order to calibrate the measured data, the signals measured for the heated sample support at reduced pressures have been used. As can be seen from the low frequency limit in Figure 3, the attenuation of the incident steady-state heat flux has changed from about 0.037 at ambient pressure to about 0.02 at a pressure of 1 mbar.

In Figure 4 and 5 the normalized phases are shown for different air pressures, the relatively higher in Figure 4

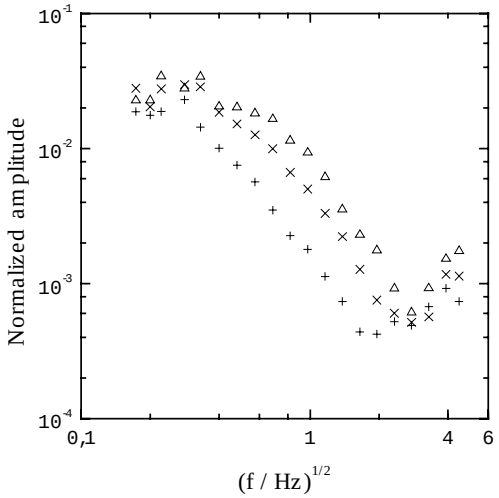

Fig. 3: Normalized amplitudes of a 2-foil / 1-spacer-layer sandwich at 20 mbar (Δ), 6 mbar (x), 1 mbar (+).

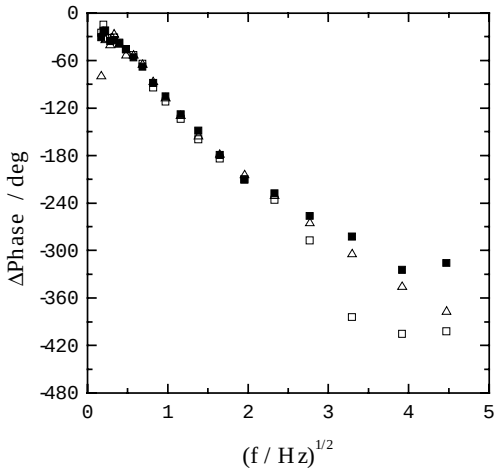

Fig. 4 : Normalized phases of a 2-foil / 1-spacer-layer sandwich at 750 mbar (■), 50 mbar (Δ), 20 mbar (□).

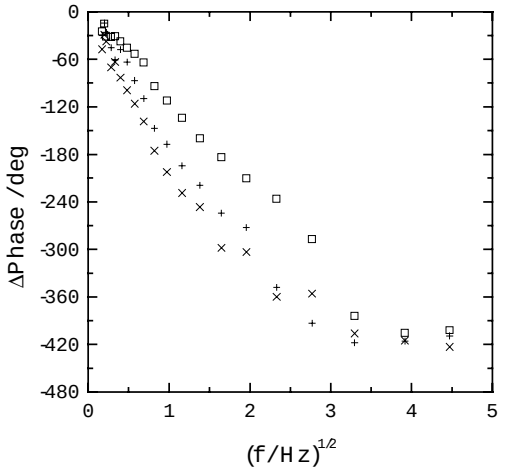

Fig. 5: Normalized phases of a 2-foil / 1-spacer-layer sandwich at 20 mbar (□), 3 mbar (+), 1.5 mbar (x).

with 750 mbar (■), 50 mbar (Δ) and 20 mbar (□), and the lower ones in Figure 5 (20 mbar (□), 3 mbar (+) and 1.5 mbar (x). In general, the normalized phases decrease with decreasing pressure, which means that the effective thermal diffusivity decreases with reducing pressure. This is in agreement with the stronger attenuation of the transmitted heat flux shown in Figure 3. Between ambient pressure and ~20 mbar, the slope of the normalized phases and the thermal diffusivity decrease very slowly, below 20 mbar this decrease is stronger. Additionally one observes, that the phases first start to decrease at higher frequencies (Fig. 4), which means at lower thermal diffusion length. At lower pressures and higher frequencies, the detection of the transmission signal is thus limited by the background fluctuation limit [2].

5 CONCLUSIONS AND OUTLOOK

The measurements, both at ambient pressure and at reduced pressures, have shown that the relative attenuation factors of steady-state heat flux can be determined by extrapolation from the measured lower frequencies, and the relative decrease of the thermal diffusivity can be determined from the intermediate frequency range. Both, the relative attenuation factor and the effective thermal diffusivity are the relevant thermal parameters to characterize thermal insulation foils.

In order to determine the absolute values of the thermal diffusivity, reference measurements of samples of well defined IR-optical and thermal properties have still to be done. As shown here the measurements can be interpreted based on the theory of thermal waves transmitted through samples of finite thickness. The radiative contributions to the heat transport have been identified only at higher modulation frequencies. This is mainly due to the fact that the thermal contact between the various mylar foils is relatively narrow. Further measurements to compare the efficiency of different types of superinsulation foils and different numbers of aluminized mylar foils are now in progress, and future measurements will have to be done, both at reduced pressures and reduced temperatures.

The technique used here in the *transmission configuration* of thermal waves to compare different foils with respect to their shielding efficiency can also be applied to control superinsulation systems under working conditions. In this case, the thermal wave technique has to be applied in the *reflection configuration*, where the thermal waves are excited and detected at the same surface.

REFERENCES

[*] kindly provided by CERN, Geneva.

[1] B.K. Bein, J. Gibkes, A. Mensing, J. Pelzl, High Temp.-High Pressures 26 (1994), 299-307.

[2] J. Bolte, J.H. Gu, B.K. Bein, High Temp.-High Pressures 29 (1997), 567-580.

[3] A.HajDaoud, PhD th. Ruhr-University Bochum,1999.